

# Epitaxial Growth of InN Films by Molecular-Beam Epitaxy Using Hydrazoic Acid (HN<sub>3</sub>) as an Efficient Nitrogen Source<sup>†</sup>

J. T. Chen,<sup>‡</sup> C. L. Hsiao,<sup>§</sup> H. C. Hsu,<sup>§</sup> C. T. Wu,<sup>||</sup> C. L. Yeh,<sup>⊥</sup> P. C. Wei,<sup>#</sup> L. C. Chen,<sup>§</sup> and K. H. Chen<sup>\*,§,+</sup>

*Graduate Institute in Electro-Optical Engineering, Tatung University, Taipei104, Taiwan, Center for Condensed Matter Sciences, National Taiwan University, Taipei 106, Taiwan, Materials Science and Engineering, National Taiwan University, Taipei106, Taiwan, Graduate Institute of Materials Science and Technology, National Taiwan University of Science and Technology, Taipei 106, Taiwan, Department of Materials Science and Engineering, National Tsing Hua University, Hsinchu 300, Taiwan, and Institute of Atomic and Molecular Sciences, Academia Sinica, Taipei 106, Taiwan*

*Received: December 27, 2006; In Final Form: March 26, 2007*

Epitaxial InN films have been successfully grown on *c*-plane GaN template by gas-source molecular-beam epitaxy with hydrazoic acid (HN<sub>3</sub>) as an efficient nitrogen source. Results in residual-gas analyzer show that the HN<sub>3</sub> is highly dissociated to produce nitrogen radicals and can be controlled in the amounts of active nitrogen species by tuning HN<sub>3</sub> pressure. A flat and high-purity InN epilayer has been realized at the temperature near 550 °C, and a growth rate of 200 nm/hr is also achieved. Moreover, the epitaxial relationship of the InN(002) on the GaN(002) is reflected in the X-ray diffraction, and the full-width at half-maximum of the InN(002) peak as narrow as 0.05° is related to a high-quality crystallinity. An infrared photoluminescence (PL) emission peak at 0.705 eV and the integrated intensity increasing linearly with excitation power suggest that the observed PL can be attributed to a free-to-bound recombination.

## Introduction

Indium nitride (InN) is considered as a very attractive material for future photonic and electronic devices owing to its outstanding properties such as smallest electron effective mass, largest mobility, highest peak and saturation velocities, and smallest direct band gap among the nitride semiconductors.<sup>1–7</sup> These excellent properties suggest that there may be distinct advantages offered by using InN in high-frequency centimeter and millimeter wave devices. Besides, the InGaN quantum wells are indispensable for light emitting devices because incorporation of small concentrations of indium in the active GaN layer increases luminescence efficiency considerably. Hence, the use of InN and its alloys with GaN and AlN makes it possible to extend the emission spectrum of nitride-based light-emitting diodes (LEDs) and laser diodes (LDs) from ultraviolet to near-infrared region.<sup>8–13</sup>

However, obtaining a high quality InN is difficult due to thermal instability of InN and large lattice mismatch between InN and common substrates.<sup>1–4</sup> Many fabrication methods, which including molecular-beam epitaxy (MBE), chemical vapor deposition (CVD), sputtering, and so on, have been used to obtain high quality InN epitaxial films.<sup>1–4,10–12</sup> Among them, thin films grown by the MBE technique show better crystalline quality, higher mobility, and lower carrier density than that

grown by other techniques.<sup>2,3</sup> Generally, N<sub>2</sub>-plasma source and ammonia are two common nitrogen sources used in the MBE technique.<sup>13,14</sup> However, the N<sub>2</sub>-plasma source needs a high cost plasma generator system, and ammonia shows a poor efficiency of producing atomic nitrogen. To meet the efficient cost and to obtain a large amount of atomic nitrogen, a high-performance nitrogen source, hydrazoic acid (HN<sub>3</sub>), is considered to be the nitrogen source for growing high-quality InN by gas-source molecular-beam epitaxy (GSMBE). Although the HN<sub>3</sub> source has been used to grow nitride semiconductors by CVD growth technique and shows good crystalline quality,<sup>15,16</sup> there are rare reports on the use of HN<sub>3</sub> to grow GaN thin film in MBE technique.<sup>17</sup> Unfortunately, the growth of epitaxial InN film is much more difficult than that of other nitride semiconductors because of its extremely low decomposition temperature of 550 °C.<sup>3</sup> Therefore, the successful demonstration in the growth of InN at low temperature is important because this source can be possible to replace the use of ammonia (NH<sub>3</sub>) in the GSMBE technique. In addition, a comparable growth rate of 200 nm/hr to an N<sub>2</sub>-plasma source shows a potential to be a useful nitrogen source for the growth of nitride semiconductors in general. In this work, we present the growth of InN films at different temperatures by MBE technique using hydrazoic acid (HN<sub>3</sub>) as an efficiency nitrogen source. No extra thermal cracker was used even when the growth temperature was as low as 250 °C. The chemical properties of HN<sub>3</sub> were characterized by temperature-dependent and pressure-dependent mass spectroscopy. Crystalline structure of InN films was investigated by in-situ reflection high-energy electron diffraction (RHEED) as well as ex-situ field-emission scanning electron microscopy (FESEM) and X-ray diffraction (XRD) analyses. Power-dependent photoluminescence (PL) spectroscopy was used to investigate the optical property of InN films.

<sup>†</sup> Part of the special issue "M. C. Lin Festschrift".

\* To whom correspondence should be addressed. P.O. Box 23-166, Taipei 10617, Taiwan; E-mail: chenkh@pub.iam.s.sinica.edu.tw, Phone: 886-2-2366-8232, Fax: 886-2-2362-0200.

<sup>‡</sup> Tatung University.

<sup>§</sup> Center for Condensed Matter Sciences, National Taiwan University.

<sup>||</sup> Materials Science and Engineering, National Taiwan University.

<sup>⊥</sup> National Taiwan University of Science and Technology.

<sup>#</sup> National Tsing Hua University.

<sup>+</sup> Academia Sinica.

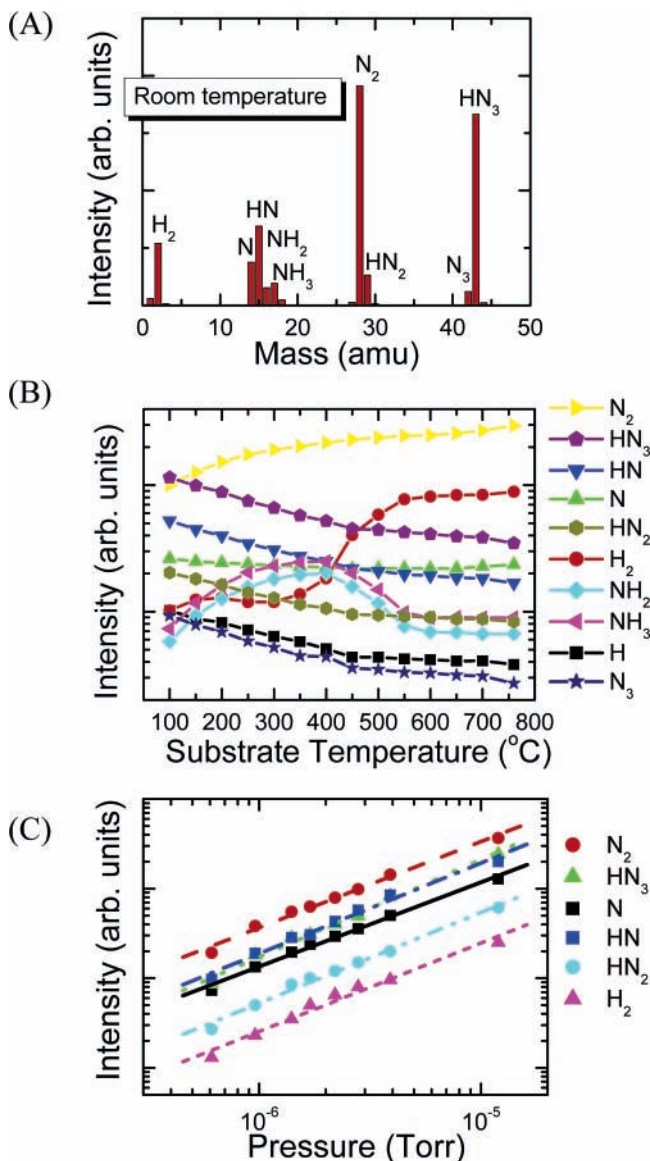


**Figure 1.** (A) RGA result of the gaseous products of thermal dissociation of hydrazoic acid at room temperature. (B) Dependence of amounts of related fragments and substrate temperature. (C) Dependence of amounts of  $HN_3$ -related fragments and  $HN_3$  partial pressure. The amounts of activated nitrogen species of  $HN_3$  exhibited a linearly controllable behavior with  $HN_3$  pressure at a given substrate temperature.

### Experimental Procedures

InN thin films were grown on the GaN template using a homemade GSMBE system, which consists of loading and growth chambers. Residual-gas analyzer (RGA), reflection high-energy electron diffraction (RHEED), and beam-flux monitor (BFM) were equipped in the growth chamber. The base pressure of the growth chamber was pumped to  $\sim 1 \times 10^{-9}$  Torr using a combination of a mechanical pump and a turbomolecular pump. The indium source was evaporated and ejected from a conventional Knudsen cell (K-cell) while the nitrogen source was supplied from highly volatile  $HN_3$  precursor during the GSMBE process.<sup>15,16</sup>  $HN_3$  was prepared in vacuum by acidification of an appropriate amount of  $NaN_3$  at room temperature in a pre-evacuated round-bottom Pyrex flask by slowly dripping 50–60%  $H_3PO_4$  solution using a funnel attached to a stopcock. The  $HN_3$  gas generated from the reaction was first passing through a large, dry ice cooled trap to remove a large amount

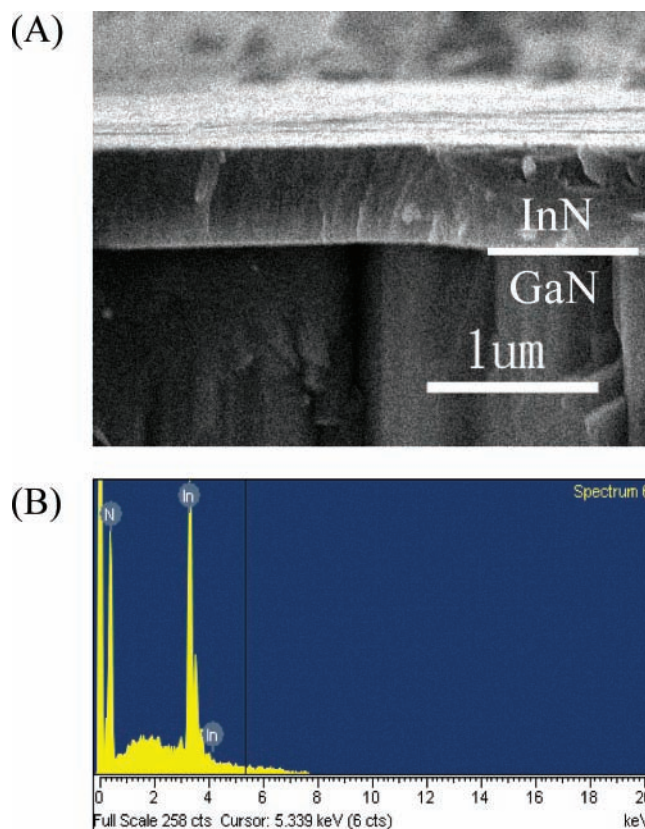


**Figure 2.** (A) Cross sectional FESEM image with tiled  $15^{\circ}$  of InN epitaxial film grown on the GaN template at  $550^{\circ}C$ . (B) EDX analysis of the InN layer.

of  $H_2O$  from the reactor. The prepurified  $HN_3$  gas was further dried by two U-shaped traps maintained at dry ice temperature before being condensed at a liquid-nitrogen U-trap. The system was subjected to continuing diffusion pumping to avoid the buildup of non-condensable gases such as  $N_2$ . The solid  $HN_3$  collected at the liquid  $N_2$ -trap, after sealing off with two high-vacuum stopcocks, was allowed to slowly heat up to room temperature and liquefy overnight. The clear liquid  $HN_3$  (which is safe to handle) was then stored at dry ice temperature for a long term use. The vapor from the liquid at dry ice temperature, about 0.7 Torr, is sufficient for chemical-beam epitaxy (CBE) or MBE applications. It should be noted that the entire  $HN_3$  generator is placed inside a hood with a protective plastic sliding door. Solid  $HN_3$  should be handled with extreme care as it is known to explode during the melting process. Therefore, despite its advantages over other nitrogen sources, the inexperienced user of  $HN_3$  is advised to contact the authors for precautions.

Prior to InN growth, the GaN template was cleaned by acetone, methanol, and D.I. water with ultrasonic bath to remove residual organic contaminations on substrate surface, and further chemically cleaned by dipping a dilute HCl solution for 5 min to remove surface native oxides. After the chemical cleaning process, the GaN template was annealed at  $800^{\circ}C$  for 30 min in the growth chamber before the growth of InN. After cooling down to  $200^{\circ}C$ , appearance of GaN surface reconstruction RHEED patterns ensured a perfect surface condition.<sup>18</sup> Afterward, various growth conditions were applied to obtain an epitaxial InN film on the GaN template, which included tuning V/III ratio and substrate temperature. Usually, InN films were deposited for 1–10 h and the growth pressure was controlled in the range of  $10^{-7}$ – $10^{-5}$  Torr. Several techniques were used to characterize the as-grown InN films, including in-situ RGA

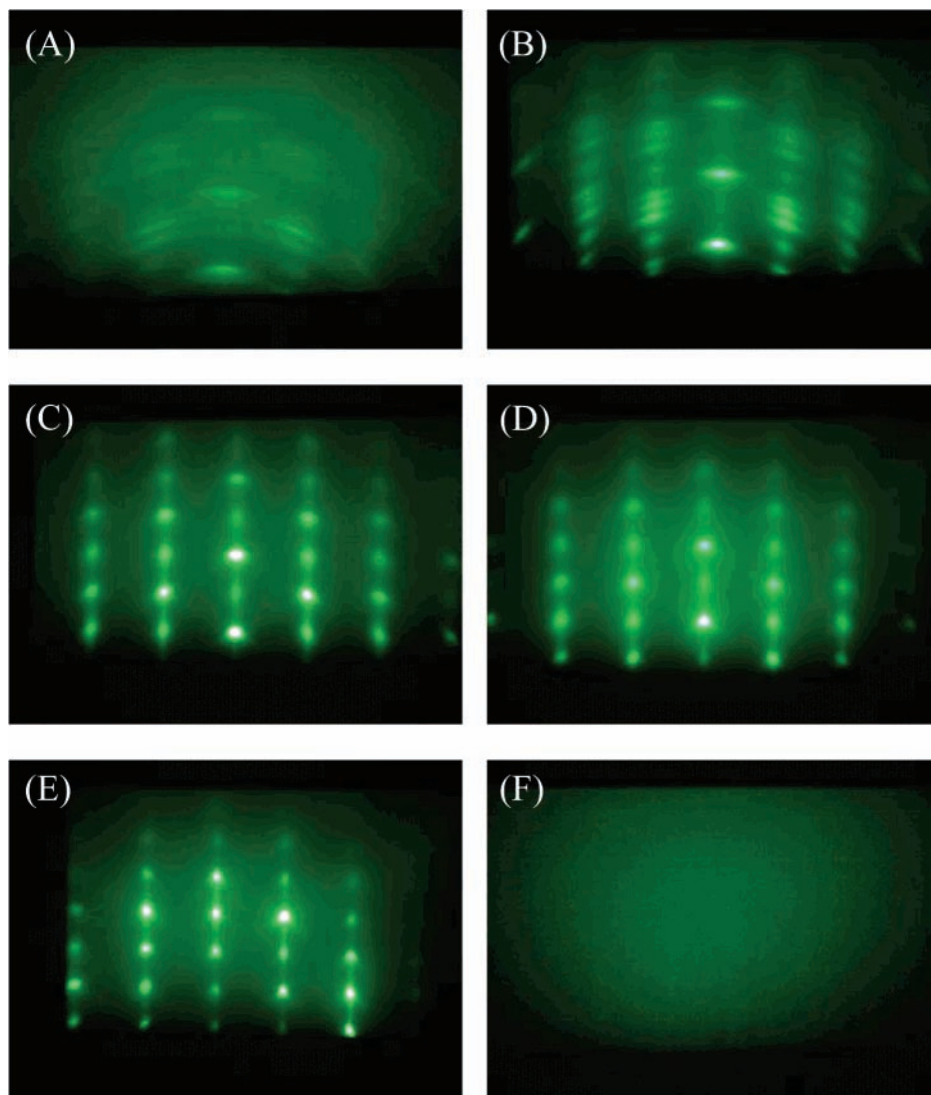


**Figure 3.** RHEED patterns taken at different growth temperature. (A) 250, (B) 350, (C) 450, (D) 500, (E) 550, and (F) 600 °C.

and RHEED, as well as ex-situ FESEM, XRD analysis, and PL spectroscopy.

### Results and Discussion

Figure 1A shows a mass spectrum of the thermal dissociation of  $\text{HN}_3$  using the RGA at substrate temperature of room temperature under the pressure of  $4.0 \times 10^{-6}$  Torr. A substantial size of  $\text{N}^+$  signals ( $m/z = 14$ ) from atomic nitrogen and related fragments such as  $\text{HN}$ ,  $\text{HN}_2$ , and  $\text{NH}_2$  were detected, which reveals  $\text{HN}_3$  has low dissociation energy and can be easily decomposed at such low temperature. The observation of these fragments is consistent with the result of infrared reflection absorption spectroscopy (IRRAS) studied by Russell et al.<sup>19</sup> Temperature-dependent mass spectrum is used to study the thermal decomposition of  $\text{HN}_3$  in the temperature range of 25–800 °C, as shown in Figure 1B. All of the  $\text{HN}_3$ -related fragments decrease and shows the same trend as increasing the substrate temperature. When temperature is lower than 300 °C, the  $\text{H}_2$  does not increase as increasing temperature but  $\text{NH}_3$ ,  $\text{NH}_2$ , and  $\text{N}_2$  fragments increase, which indicates that the decomposed  $\text{HN}_3$ -related fragments form ammonia ( $\text{NH}_3$ ) related fragments not  $\text{H}_2$ . When temperature is higher than 400 °C, a large amount of  $\text{H}_2$  was produced and the  $\text{NH}_3$ -related fragments decrease dramatically. Until the temperature higher than 600 °C, all the

species are in a balanced status. From above results, the data indicates that the decomposed  $\text{HN}_3$ -related fragments form either  $\text{NH}_3$ -related fragments or  $\text{N}_2$  and  $\text{H}_2$  species. Active nitrogen species, such as  $\text{HN}$  and  $\text{N}$ , still follow the trend of  $\text{HN}_3$ -related fragments. Hence, the V/III ratio at a stoichiometric condition, a very important parameter in MBE growth, can still be controlled by tuning the  $\text{HN}_3$  partial pressure at different substrate temperature from the trend of  $\text{HN}_3$ -related fragments, which is shown in the temperature-dependent mass spectrum.

A further study on the dependence of  $\text{HN}_3$  partial pressure and amounts of main fragments is shown in Figure 1C. The amounts of these fragments show nearly linear increase as increasing the  $\text{HN}_3$  partial pressure. Compared with other nitrogen source generated by RF plasma, in which amount of atomic nitrogen is controlled nonlinearly by plasma power,<sup>20</sup> while the amounts of reactive nitrogen species of  $\text{HN}_3$  exhibited a linearly controllable behavior with  $\text{HN}_3$  pressure at a given substrate temperature. This result can be an advantage in manipulation of growth process. Therefore, through the use of  $\text{HN}_3$ , it is possible to decrease the typical V/III ratio as low as 100, whereas other growth techniques utilizing  $\text{NH}_3$  as the nitrogen source needs a very high V/III ratio of 40 000, and a high growth temperature (>700 °C) is necessary to decompose the  $\text{NH}_3$  reagent.<sup>14,21</sup> Both conditions of high V/III ratio and

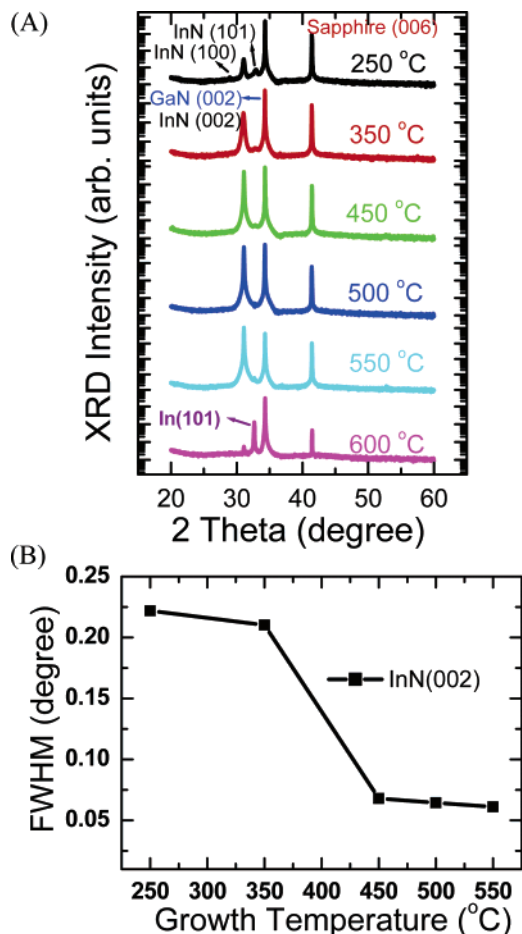


**Figure 4.** (A) XRD  $\theta/2\theta$  scan of the InN films grown on GaN templates at different growth temperature. (B) A plot of the fwhm of InN(002) vs growth temperature.

high growth temperature limit the growth of a high-quality InN film using the MBE technique.<sup>1–3</sup> Besides, comparing with  $\text{NH}_3$ , the lower atomic ratio of hydrogen/nitrogen in  $\text{HN}_3$  and the use of the lower V/III flux ratio during growth with  $\text{HN}_3$ , the excess hydrogen by product in the growth atmosphere is vastly reduced. This may possibly attributed to suppression of the hydrogen passivation of acceptors, which is believed to be one of the possible reasons of intrinsic n-type conductivity.<sup>22</sup> Hence, the use of  $\text{HN}_3$  as an efficient nitrogen source can be an excellent candidate to grow high quality nitride semiconductors.

Figure 2A shows a typical cross sectional SEM image of a flat InN layer grown on the GaN template at 550 °C. The as-grown InN film on the GaN template shows a continuous growth without voids appeared at interface, which indicates a well coalescence in grain boundaries at initial growth. In addition, the composition of InN film was determined by energy dispersive X-ray spectroscopy (EDX) as shown in Figure 2B. Only In and N elements appear in the spectrum and no any noticeable contaminants such as oxygen, carbon, or other impurities are detected, which indicates that high-purity InN film has been grown by  $\text{HN}_3$ -source MBE. A similar observation was reported previously by Bu et al.<sup>16</sup> In order to further study the growth behavior of InN using  $\text{HN}_3$  source, InN films were grown at different substrate temperatures. From RHEED patterns, as shown in Figure 3, the InN film grown at low temperature of 250 °C reveals a ring-like pattern and becomes a streaky-like pattern as increasing substrate temperature to 450 °C, implying the surface changes from rough with poor crystalline quality to smooth with better quality at increasing

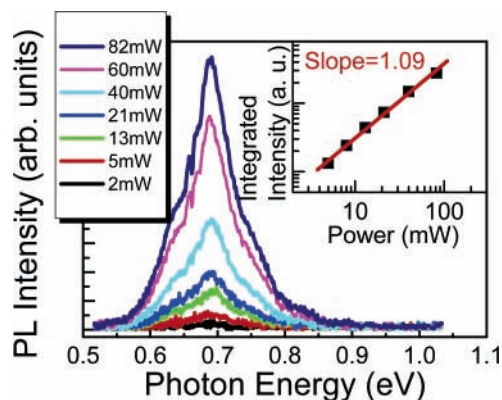


**Figure 5.** Power dependent PL spectra of InN epitaxial film measured at room temperature. The inset shows the plot of integrated PL intensity vs excitation power.

growth temperature. On the contrary, a blurred pattern appears while raising the growth temperature to 600 °C as a result of to the formation of indium metal on the substrate surface. It is consistent with the result of thermal decomposition of InN when the growth temperature is higher than 550 °C.<sup>2,3</sup>

The crystalline quality of InN is investigated by XRD analysis, and a semilogarithmic diagram of  $\theta/2\theta$  scan XRD is plotted to recognize some weak signals from the off-axis crystal plane, as shown in Figure 4A. At lower growth temperature of 250 °C, besides a prominent on-axis InN(002) peak at 31.3° in the pattern, there are two small peaks appeared at 29.1 and 33.2° are corresponding to the off-axis crystal planes of InN(100) and InN(101) of wurtzite InN (Joint Committee on Powder Diffraction Standards (JCPDS) 02-1450), respectively.<sup>12</sup> Although the low-temperature-grown InN film shows a bit polycrystalline phase, no In(101) signal at 32.9° is shown in the XRD pattern. This significant result implies that the indium and nitrogen, which is provided by  $\text{HN}_3$  source, can be completely reacted even at the growth temperature as low as 250 °C. When the growth temperature is in the range of 450–550 °C, the XRD signals show only InN(002), GaN(002) at 34.6°, and  $\text{Al}_2\text{O}_3$ -(006) at 41.4° without any extra off-axis InN crystal plane, indicating that InN films are wurtzite structure and are grown along the *c*-axis direction with a high crystallinity. As the growth temperature increasing to 600 °C, a dominated In(101) diffraction peak appearance indicates that the InN cannot be grown at temperature higher than its decomposition temperature. This result is in agreement with the pervious observation from RHEED. To further investigate the crystalline quality, the full-width at half-maximum (fwhm) of InN(002) peak versus growth temperature is plotted in Figure 4B. As the thermal dynamic prediction, the crystalline quality becomes better as increasing growth temperature to its decomposition temperature. A narrow fwhm of 0.06° is obtained when InN film was grown at 550 °C. Furthermore, the X-ray rocking curve analysis was used to examine the mosaicity of the InN film. A narrow fwhm of 0.31° is also obtained on a 350 nm thick InN film, indicating a good crystalline quality with a low misorientation subgrains in the film.<sup>23</sup> In addition, owing to the high dissociation of  $\text{HN}_3$ , the efficiency of the InN growth is much increased. While the fluxes of indium and  $\text{HN}_3$  were increased simultaneously, the growth rate up to about 200 nm per hour was also achieved.

The PL measurement was taken from a 0.5 m monochromator equipped with a 300 gr/mm grating and an extend-InGaAs detector (detecting range: 0.5–1.1 eV) using a frequency-doubled  $\text{Nd}^{3+}$ -YAG laser at 532 nm as the excitation source. Figure 5 shows power-dependent PL spectra measured at room

temperature from an InN film grown at 550 °C. The emission peak is at 0.705 eV with a fwhm of 118 meV, which is consistent with the emission of most reports in the range of 0.6–0.8 eV in recent for InN epilayers as well as one-dimensional InN nanostructures<sup>2,3,10–12</sup>. The inset of the Figure 5 shows the dependence of excitation power and PL integrated intensity of the InN film. The integrated PL intensity increases linearly with the excitation power near 2 orders of magnitude and shows no saturation even at the highest excitation power of 82 mW. The emission originates from the free electrons above the conduction band to holes localized in the valance band tail (free-to-bound recombination) as reported in recent literature.<sup>24,25</sup>

## Conclusion

We have demonstrated the use of  $\text{HN}_3$  reagent as an efficient nitrogen source for growing high-quality InN film in GSMBE. Both the crystalline quality and the growth rate are comparable with the radio frequency MBE technique. FESEM image shows that a flat and smooth InN thin film has been realized. The XRD analyses demonstrate that epitaxial InN thin film with wurtzite structure grown along  $c$ -plane direction and epitaxial relationship between InN and GaN is  $\text{InN}(002)//\text{GaN}(002)$  and the fwhm of the  $\text{InN}(002)$  peak is as narrow as  $0.06^\circ$ . Furthermore, the grown InN film shows the IR-PL emission peak of 0.705 eV at room temperature, which can be attributed to a free-to-bound emission. These findings reveal that  $\text{HN}_3$  has a great potential to be an alternative nitrogen source in the growth of high-quality nitride semiconductors. Therefore, we believe that the  $\text{HN}_3$  could be a high-performance nitrogen source, which can be applied to other growth techniques, such as MOVPE, HVPE, etc.

**Acknowledgment.** The authors acknowledge the financial support from the National Science Council(NSC), Ministry of Education, Academia Sinica, Taiwan, and Asian Office of Aerospace Research and Development under AFOSR. We are grateful to Prof. M. C. Lin for the construction of the  $\text{HN}_3$  generator and the detailed procedure employed for preparation and purification of the  $\text{HN}_3$ .

## References and Notes

(1) Davydov, V. Y.; Klochikhin, A. A.; Seisyan, R. P.; Emtsev, V. V.; Ivanov, S. V.; Bechstedt, F.; Furthmüller, J.; Harima, H.; Murdryi, A. V.; Aderhold, J.; Semchinova, O.; Graul, J. *Phys. Status Solidi B* **2002**, *229*, R1.

- (2) Wu, J.; Walukiewicz, W.; Yu, K. M.; Arger, J. W., III; Haller, E. E.; Lu, H.; Schaff, W. J.; Saito, Y.; Nanishi, Y. *Appl. Phys. Lett.* **2002**, *80*, 3967.
- (3) Nanishi, Y.; Saito, Y.; Yamaguchi, T. *Jpn. J. Appl. Phys.* **2003**, *42*, 2549.
- (4) Tansley, T. L.; Foley, C. P. *J. Appl. Phys.* **1986**, *59*, 3241.
- (5) Mohammad, S. N.; Morkoc, H. *Prog. Quantum Electron.* **1996**, *20*, 361.
- (6) Chin, V. W. L.; Tansley, T. L.; Osotchan, T. *J. Appl. Phys.* **1994**, *75*, 7365.
- (7) Foutz, B. E.; O'leary, S. K.; Shur, M. S.; Eastman, L. F. *J. Appl. Phys.* **1999**, *85*, 7727.
- (8) Shi, S. C.; Chen, C. F.; Chattopadhyay, S.; Lan, Z. H.; Chen, K. H.; Chen, L. C. *Adv. Funct. Mater.* **2005**, *15*, 781.
- (9) Tu, L. W.; Hsiao, C. L.; Chi, T. W.; Lo, I.; Hsieh, K. Y. *Appl. Phys. Lett.* **2003**, *82*, 1601.
- (10) Hsiao, C. L.; Tu, L. W.; Chen, M.; Jiang, Z. W.; Fan, N. W.; Tu, Y. J.; Wang, K. R. *Jpn. J. Appl. Phys.* **2005**, *44*, L1076.
- (11) Gwo, S.; Wu, C. L.; Shen, C. H.; Chang, W. H.; Hsu, T. M.; Wang, J. S.; Hsu, J. T. *Appl. Phys. Lett.* **2004**, *84*, 3765.
- (12) Hu, M. S.; Wang, W. M.; Chen, T. T.; Hong, L. S.; Chen, C. W.; Chen, C. C.; Chen, Y. F.; Chen, K. H.; Chen, L. C. *Adv. Funct. Mater.* **2006**, *16*, 537.
- (13) Hsiao, C. L.; Tu, L. W.; Chi, T. W.; Seo, H. W.; Chen, Q. Y.; Chu, W. K. *J. Vac. Sci. Technol., B* **2006**, *24*, 845.
- (14) Tang, H.; Webb, J. B. *Appl. Phys. Lett.* **1999**, *74*, 2373.
- (15) Chtchekine, D. G.; Fu, L. P.; Gilliland, G. D.; Chen, Y.; Ralph, S. E.; Bajaj, K. K.; Bu, Y.; Lin, M. C.; Bacalzo, F. T.; Stock, S. R. *J. Appl. Phys.* **1997**, *81*, 2197.
- (16) Bu, Y.; Ma, L.; Lin, M. C. *J. Vac. Sci. Technol., A* **1993**, *11*, 2931.
- (17) Oberman, D. B.; Lee, H.; Götz, W. K.; Harris, J. S., Jr. *J. Cryst. Growth* **1995**, *150*, 912.
- (18) Smith, A. R.; Feenstra, R. M.; Greve, D. W.; Shin, M. S.; Skowronski, M.; Neugebauer, J.; Northrup, J. E. *Appl. Phys. Lett.* **1998**, *72*, 2114.
- (19) Russell, J. N.; Bermudez, V. M.; Leming, A. *Langmuir* **1996**, *12*, 6492.
- (20) Schenk, H. P. D.; Kipshidze, G. D.; Kaiser, U.; Fissel, A.; Kräußlich, J.; Schulze, J.; Richter, W. *J. Cryst. Growth* **1999**, *200*, 45.
- (21) Baillargeon, J. N.; Cheng, K. Y.; Jackson, S. L.; Stillman, G. E. *J. Appl. Phys.* **1991**, *69*, 8025.
- (22) Davis, E. A.; Cox, S. F. J.; Lichti, R. L.; Van de Walle, C. G. *Appl. Phys. Lett.* **2003**, *82*, 592.
- (23) Cullity, B. D.; Stock, S. R. *Elements of X-ray Diffraction*, 3rd ed.; Prentice Hall: Upper Saddle River, NJ, 2001; Chapter 17, p 524.
- (24) Arnaudov, B.; Paskova, T.; Paskov, P. P.; Magnusson, B.; Valcheva, E.; Monemar, B.; Lu, H.; Schaff, W. J.; Amano, H.; Akasaki, I. *Phys. Rev. B* **2004**, *69*, 115216.
- (25) Fu, S. P.; Chen, Y. F.; Tan, K. W. *Solid State Commun.* **2006**, *137*, 203.